BELLE2-CONF-PH-2020-002
April 15, 2020

Measurement of the branching fraction $\mathcal{B}(\bar{B}^0 \to D^{*+}\ell^-\bar{\nu}_\ell)$ with early Belle II data

(The Belle II Collaboration)

Abstract

We measure the branching fractions for the decays $\overline{B}^0 \to D^{*+}e^-\overline{\nu}_e$ and $\overline{B}^0 \to D^{*+}\mu^-\overline{\nu}_\mu$ using 8.70 ± 0.09 fb^{-1} of data collected by the Belle II experiment at the SuperKEKB asymmetric-energy e^+e^- collider. Candidate signal decays are reconstructed with the subsequent decays $D^{*+} \to D^0\pi^+$ and $D^0 \to K^-\pi^+$. We obtain the results $\mathcal{B}(\overline{B}^0 \to D^{*+}e^-\overline{\nu}_e) = (4.55 \pm 0.14(\text{stat}) \pm 0.35(\text{sys}))\%$ and $\mathcal{B}(\overline{B}^0 \to D^{*+}\mu^-\overline{\nu}_\mu) = (4.84 \pm 0.13(\text{stat}) \pm 0.37(\text{sys}))\%$, in agreement with the world average. The measurement serves to validate the full chain of detector operation and calibration, data collection and processing, and production of physics results in the case of semileptonic B-meson decays.

1. INTRODUCTION

The decays $\overline{B}^0 \to D^{*+}\ell^-\overline{\nu}_l$ (where $\ell = e$ or μ) are important for measuring the magnitude of the Cabibbo-Kobayashi-Maskawa matrix element $|V_{cb}|$ and for understanding the hadronic dynamics of B decays. They also constitute a source of background for charmless semileptonic decays and for the study of $\overline{B}^0 \to D^{(*)+}\tau^-\overline{\nu}_\tau$. All this motivates precise measurements of their branching fractions and kinematic distributions.

The most precise measurements of $\mathcal{B}(\overline{B}^0 \to D^{*+}\ell^-\overline{\nu}_l)$ were obtained by the *BABAR* [1] and Belle [2] collaborations with data sets recorded a decade ago. Since March 2019, the Belle II experiment has been collecting e^+e^- collision data with the full detector. The integrated luminosity is still much smaller than those of the previous-generation B factories, *BABAR* and Belle. However, this measurement of $\mathcal{B}(\overline{B}^0 \to D^{*+}\ell^-\overline{\nu}_l)$ serves to validate the full analysis chain, from detector operation and calibration, through data collection and processing, to production of physics results, including systematic uncertainties.

2. THE BELLE II DETECTOR AND DATA SAMPLE

The Belle II detector [3, 4] operates at the SuperKEKB asymmetric-energy, electron-positron collider [5], located at the KEK laboratory in Tsukuba, Japan. The detector consists of several detector subsystems arranged around the beam pipe in a cylindrical geometry.

The innermost subsystem is the vertex detector, which includes two layers of silicon pixel detectors and four outer layers of silicon strip detectors. Currently, the second pixel layer is installed in only a small part of the solid angle, and the remaining vertex detector layers are fully installed. Most of the tracking volume is covered by a helium and ethane-based, small-cell drift chamber.

Outside the drift chamber, a Cherenkov-light imaging and time-of-propagation detector provides charged-particle identification in the barrel region. In the forward endcap, this function is provided by a proximity-focusing, ring-imaging Cherenkov detector with an aerogel radiator. Further out is an electromagnetic calorimeter, consisting of a barrel and two endcap sections made of CsI(Tl) crystals. A uniform 1.5 T magnetic field is provided by a solenoid situated outside the calorimeter. Multiple layers of scintillators and resistive plate chambers, inserted between the magnetic flux-return iron plates, constitute the K_L and muon identification system.

The data used in this analysis were collected at a center-of-mass (CM) energy of 10.58 GeV, corresponding to the mass of the $\Upsilon(4S)$ resonance. The energies of the electron and positron beams are 7 GeV and 4 GeV, respectively, resulting in a boost of $\beta\gamma = 0.28$ of the CM frame relative to the lab frame. The integrated luminosity of the data is 8.70 ± 0.09 fb^{-1}.

Simulated Monte Carlo (MC) samples of signal events containing 10^5 events for each of $\overline{B}^0 \to D^{*+}e^-\overline{\nu}_e$ and $\overline{B}^0 \to D^{*+}\mu^-\overline{\nu}_\mu$, with the subsequent decays $D^{*+} \to D^0(\to K^-\pi^+)\pi^+$, are used to obtain the reconstruction efficiencies and signal kinematic distributions. These events were generated with EvtGen [6]. Samples of background events are used to obtain

kinematic distributions of the background. These include a sample of $e^+e^- \to B\bar{B}$ with generic B-meson decays, generated with EvtGen, and corresponding to an integrated luminosity of 100 fb^{-1}. A 100 fb^{-1} sample of continuum $e^+e^- \to q\bar{q}$ ($q = u, d, s, c$) is simulated with KK2f [7] interfaced with PYTHIA [8].

3. EVENT SELECTION

We reconstruct candidate $\overline{B}^0 \to D^{*+}\ell^-\overline{\nu}_l$ decays, with the subsequent decays $D^{*+} \to D^0\pi_s^+$, $D^0 \to K^-\pi^+$. Here, π_s indicates the soft pion originating from the D^{*+} decay. Reconstruction of the charge-conjugate decays is implied.

Signal candidate reconstruction begins with the selection of 4 charged-particle tracks. The distance between each track and the interaction point is required to be less than 0.5 cm in the $r - \phi$ plane and less than 2 cm along the z direction. All tracks except the π_s candidate must have at least one hit in the drift chamber. The lepton candidate must have a CM frame momentum in the range $p^*_\ell \in [1.2, 2.4]$ GeV/c. It must also satisfy lepton-identification (lepton-ID) criteria based on information from all available detectors. Given the high purity of the decay chain, application of kaon or pion identification criteria is deemed unnecessary and is thus not performed.

A vertex fit is applied to the D^0 candidate, constraining its $K^-\pi^+$ daughter tracks to originate from the same point. The invariant mass of the D^0 candidate is required to satisfy $m_{K\pi} \in [1.85, 1.88]$ GeV/c^2 after the fit. The $D^{*+} \to D^0\pi_s^+$ candidate decay is also subjected to a vertex fit, after which the mass difference between the D^* and D^0 candidates is required to satisfy $\Delta m \in [0.144, 0.148]$ GeV/c^2.

Continuum background is suppressed by requiring the momentum of the D^* candidate in the CM frame to be less than 2.5 GeV/c. Further continuum suppression is achieved by requiring $R_2 < 0.3$, where R_2 is the ratio of the second and zeroth Fox-Wolfram moments [9], calculated using all the tracks and photon candidates in the event.

After applying all the selection criteria above, multiple $\overline{B}^0 \to D^{*+}\ell^-\overline{\nu}_l$ candidates are found in about 1% of the events. In these events we perform a vertex fit for the decay $\overline{B}^0 \to D^{*+}\ell^-\overline{\nu}_l$ and select the candidate with the smallest value of the vertex-fit χ^2. The signal efficiency after all selection criteria is $(19.8 \pm 1.8)\%$ for $\overline{B}^0 \to D^{*+}e^-\overline{\nu}_e$ and $(21.4 \pm 2.2)\%$ for $\overline{B}^0 \to D^{*+}\mu^-\overline{\nu}_\mu$, respectively. These values are obtained from signal MC with lepton-ID efficiency corrections obtained from data-MC comparisons of reconstructed $J/\psi \to \ell^+\ell^-$ decays. The quoted uncertainties are dominated by the uncertainties on this correction, and also include the much smaller MC-statistical uncertainty.

4. SIGNAL YIELD EXTRACTION

For each candidate, we calculate the quantity

$$\cos\theta_{BY} \equiv \frac{2E^*_B E^*_Y - M^2_B - m^2_Y}{2|p^*_B||p^*_Y|}, \tag{1}$$

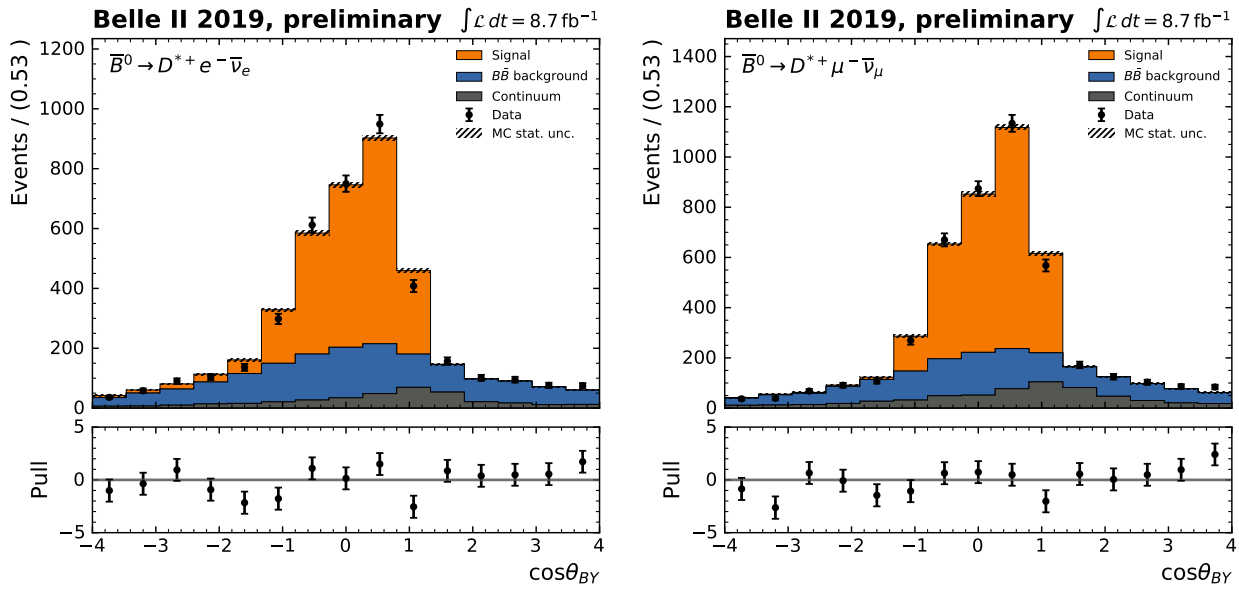

FIG. 1. Post-fit $\cos\theta_{BY}$ distributions for the selected $\overline{B}^0 \to D^{*+}e^-\overline{\nu}_e$ (left) and $\overline{B}^0 \to D^{*+}\mu^-\overline{\nu}_\mu$ (right) candidates (data points), overlaid with the signal, $B\bar{B}$ background, and continuum PDFs used in the fit as obtained from simulated MC events (histograms). The pull distributions show the difference between the data and total PDF divided by the square root of the number of data events in each bin.

where E_Y^*, $|p_Y^*|$, and m_Y are the CM energy, momentum, and invariant mass of the $D^*\ell$ system, M_B is the nominal B mass [10], and E_B^*, $|p_B^*|$ are the CM energy and momentum of the B, inferred from the CM machine energy. For correctly reconstructed $\overline{B}^0 \to D^{*+}\ell^-\overline{\nu}_l$ candidates with perfect detector resolution and correct values of E_B^* and p_B^*, $\cos\theta_{BY}$ is the cosine of the angle between the momentum of the B meson and that of the $D^*\ell$ system in the CM frame. Given the finite beam-energy spread, final-state radiation, and detector resolution, the $\cos\theta_{BY}$ distribution of signal events extends beyond the range $[-1, 1]$. The $\cos\theta_{BY}$ distributions of data and MC events are shown in Fig. 1.

We obtain the event yields N_s, N_B, and N_c for signal, $B\bar{B}$ background, and continuum, respectively, from a binned, extended-maximum-likelihood fit to the $\cos\theta_{BY}$ distribution of the data. The probability density function (PDF) used in the fit is the sum of the PDFs of these three event categories. These PDFs are obtained from the MC samples, after application of momentum- and polar-angle-dependent corrections to the lepton-identification efficiencies of leptons and hadrons. For leptons, corrections of the order of a few percent are obtained from $J/\psi \to \ell^+\ell^-$ ($\ell = e, \mu$) decays. Corrections for hadrons misidentified as leptons, obtained from samples of reconstructed $D^0 \to K^-\pi^+$ decays, are of order 1 in some regions. Applying these corrections to the PDFs changes the signal yield from the fit by 0.5% for $\overline{B}^0 \to D^{*+}e^-\overline{\nu}_e$ and by 0.1% for $\overline{B}^0 \to D^{*+}\mu^-\overline{\nu}_\mu$.

The fit results are shown in Fig. 1 and summarized in Table I.

Event type	$\overline{B}^0 \to D^{*+} e^- \overline{\nu}_e$ Yield	$\overline{B}^0 \to D^{*+} \mu^- \overline{\nu}_\mu$ Yield
N_s (Signal)	2199 ± 69	2525 ± 68
N_{B^0} ($B\bar{B}$)	1377 ± 123	1306 ± 129
N_c (Continuum)	369 ± 106	597 ± 116

TABLE I. Signal, $B\bar{B}$, and continuum event yields obtained from the fits shown in Fig. 1. The shown uncertainty is statistical only.

The branching fraction is obtained from the signal yield via

$$\mathcal{B}(\overline{B}^0 \to D^{*+} \ell^- \overline{\nu}_l) = \frac{N_s}{\epsilon \times N_{B^0} \times \mathcal{B}(D^{*+} \to D^0 \pi^+) \times \mathcal{B}(D^0 \to K^- \pi^+)}\,, \tag{2}$$

where ϵ is the product of the signal reconstruction efficiency and acceptance, and N_{B^0} is the number of B^0 mesons in the data sample, further discussed in section 5.

5. SYSTEMATIC UNCERTAINTIES AND CROSS CHECKS

The relative systematic uncertainties affecting the measurement are listed in Table II. We assume no correlation between the individual sources of uncertainty and sum them in quadrature to obtain the total systematic uncertainty. The methods used for obtaining these uncertainties are described below.

Source	Relative uncertainty (%)	
	$\overline{B}^0 \to D^{*+} e^- \overline{\nu}_e$	$\overline{B}^0 \to D^{*+} \mu^- \overline{\nu}_\mu$
Lepton-ID, PDF	0.09	0.08
MC statistics, PDF	0.64	0.55
$\mathcal{B}(\bar{B} \to D^{**} \ell \bar{\nu})$	0.18	0.08
Efficiency momentum dependence	0.1	0.1
PDF binning	0.5	0.5
Lepton-ID, efficiency	1.8	2.2
MC statistics, efficiency	0.13	0.13
Tracking of K, π, ℓ	2.5	2.5
Tracking of π_s	6.0	6.0
N_{B^0}	3.3	3.3
Charm branching fractions	1.1	1.1
Total	7.64	7.73

TABLE II. Summary of the relative systematic uncertainties for the measurements of $\mathcal{B}(\overline{B}^0 \to D^{*+} \ell^- \overline{\nu}_l)$. The first five uncertainties impact the extracted signal yield, while the others impact the other factors of Eq. (2)

The lepton-identification corrections are measured with statistical uncertainties that arise

from the limited size of the control samples, as well as systematic uncertainties. We produce 500 sets of correction values sampled from Gaussian distributions that reflect these uncertainties, accounting for systematic correlations. Each set of corrections is used to produce new MC PDFs that are used to refit the data $\cos\theta_{BY}$ distribution. The standard deviation of the distribution of the signal yield obtained with the 500 sets is 2 events for both $\overline{B}^0 \to D^{*+}e^-\overline{\nu}_e$ and $\overline{B}^0 \to D^{*+}\mu^-\overline{\nu}_\mu$. This value is thus used as the associated systematic uncertainty on the signal yield. The same procedure is used to calculate the correction on the absolute lepton-identification efficiency affecting the overall signal efficiency.

The impact of the finite sizes of the MC samples on the fit result is evaluated by varying the MC PDFs bin-by-bin according to Poisson distributions, and repeating the fit 500 times. We take the standard deviation of the resulting signal-yield distribution to estimate the systematic uncertainty.

The semileptonic decays $\bar{B} \to D^{**}\ell\bar{\nu}$, where D^{**} indicates an excited charm meson heavier than the D^*, have a similar particle content to that of signal decays. As a result, the fit may be biased if the branching fractions of $\bar{B} \to D^{**}\ell\bar{\nu}$ are incorrect in the generic MC sample. To estimate the systematic uncertainty, we obtain the $B\bar{B}$ PDF from the MC after varying the branching fractions for these decays by $\pm 25\%$, which is twice the relative uncertainty on $\mathcal{B}(\bar{B} \to D^0\pi^+\ell^-\bar{\nu})$. The resulting change in the signal yield is taken as the systematic uncertainty.

Further Data-MC differences in the reconstruction efficiency as a function of the momenta p_ℓ and p_{π_s} of the lepton and soft-pion may affect the $\cos\theta_{BY}$ PDFs and hence the signal yield. Fig. 2 shows the p_ℓ and p_{π_s} distributions in the CM frame for data and MC, with the corresponding distributions of the pull $(N_{\rm data} - N_{\rm MC})/\sqrt{N_{\rm data}}$ in each bin. The χ^2 per degrees of freedom of the pull distributions is $\chi^2/N_{\rm DOF} = 1.6$ for Fig. 2a, b, c, and 3.1 for Fig. 2d, where $N_{\rm DOF} = 9$. To test the impact of this relative disagreement on the fit, we reproduce the $\cos\theta_{BY}$ PDFs after reweighting each MC event so as to obtain $\chi^2/N_{\rm DOF} = 1$ in the p_{π_s} and p_ℓ pull distributions. Using these modified PDFs to perform the fit leads to a maximal change in the fit yield of 0.1%, which is taken as a systematic uncertainty.

The systematic uncertainty due to the choice of the number of bins in the PDF is estimated to be 0.5% by varying the number of bins up to 40.

The tracking efficiency uncertainty for the lepton, kaon, and pion is 0.82% per track. This is obtained by comparing $R_{2/3}$ for $e^+e^- \to \tau^+\tau^-$ events in data and MC, where $R_{2/3}$ is the fraction of 3-prong τ decays in which only two hadron tracks are found. The uncertainty on the soft pion tracking efficiency, 6.0%, is calculated as 20% of the inefficiency obtained from MC. The value of 20% is taken from data-MC comparison studies performed with high-momentum tracks.

To obtain the number of B^0 mesons in the sample, we use the relation

$$N_{B^0} = \mathcal{L} \times \sigma(e^+e^- \to B\bar{B}) \times \frac{f^{00}}{f^{+-}}\,. \tag{3}$$

Here $\mathcal{L}$ denotes the integrated luminosity, measured to be 8.70 ± 0.09 fb^{-1} using $e^+e^- \to e^+e^-$ and $e^+e^- \to \gamma\gamma$ events [11]. The factor $f^{+-}/f^{00} = 1.058\pm0.024$ is the ratio between fractions of charged and neutral B mesons produced in $\Upsilon(4S)$ decays [12]. We take the effective cross section $\sigma(e^+e^- \to B\bar{B})$ to be 1.110 ± 0.008 nb from measurements of $N_{B\bar{B}}$ [13] and the integrated luminosity [14] at the *BABAR* experiment. We assign an additional uncertainty of

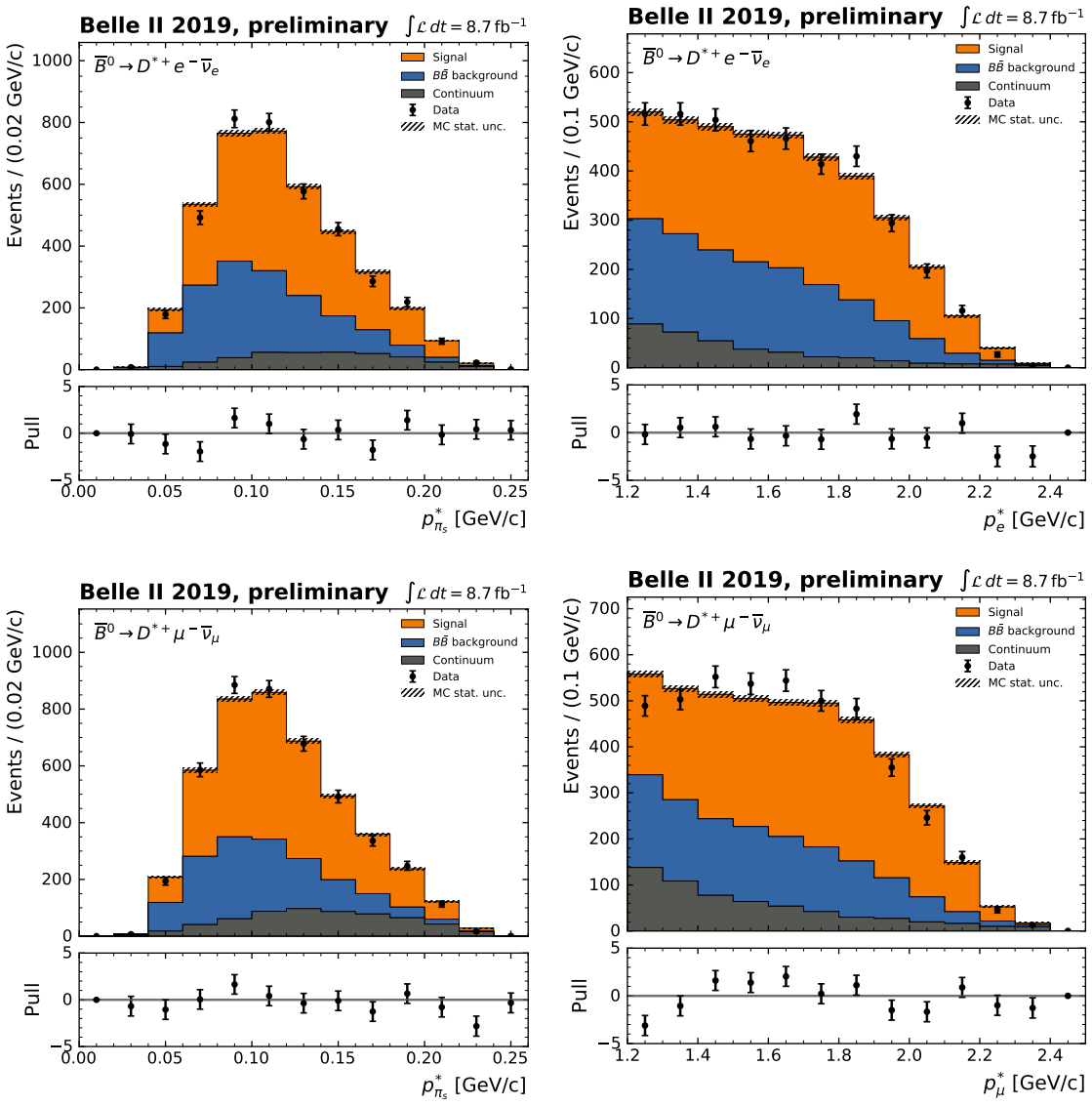

FIG. 2. Distribution of the CM momentum of the slow pion (left plots) and lepton (right plots) for the $\overline{B}^0 \to D^{*+} e^- \overline{\nu}_e$ (top plots) and $\overline{B}^0 \to D^{*+} \mu^- \overline{\nu}_\mu$ (bottom plots) modes. The data distributions are overlaid with the MC PDFs, scaled according to the fit results.

2% on this value, to account for the possibility that the average SuperKEKB CM energy is off the $\Upsilon(4S)$ resonance by up to 1.5 MeV.

Lastly, we account for the impact of the uncertainties in the charm branching fractions, $\mathcal{B}(D^{*+} \to D^0 \pi^+) = (67.7 \pm 0.5)\%$ and $\mathcal{B}(D^0 \to K^- \pi^+) = (3.950 \pm 0.031)\%$ [10], on the signal branching fraction.

6. BRANCHING FRACTION RESULTS AND SUMMARY

From Eq. (2) we measure for the $\overline{B}^0 \to D^{*+}\ell^-\overline{\nu}_l$ branching fractions:

$$\mathcal{B}(\overline{B}^0 \to D^{*+}e^-\overline{\nu}_e) = (4.55 \pm 0.14(\text{stat}) \pm 0.35(\text{sys}))\% \,, \tag{4}$$
$$\mathcal{B}(\overline{B}^0 \to D^{*+}\mu^-\overline{\nu}_\mu) = (4.84 \pm 0.13(\text{stat}) \pm 0.37(\text{sys}))\% \,. \tag{5}$$

Considering the statistical uncertainties only, the branching fractions for the two modes are consistent to within 1.5 standard deviations.

In summary, we measure the branching fractions of the decays $\overline{B}^0 \to D^{*+}e^-\overline{\nu}_e$ and $\overline{B}^0 \to D^{*+}\mu^-\overline{\nu}_\mu$ using 8.7 fb^{-1} of data collected by the Belle II experiment in 2019. The world average value of the branching fraction $\mathcal{B}(\overline{B}^0 \to D^{*+}\ell^-\overline{\nu}_l) = (5.05\pm0.14)\%$ [10] was obtained with a different value of the D^0 branching fraction, $\mathcal{B}(D^0 \to K^-\pi^+) = (3.89 \pm 0.04)\%$. Accounting for this difference, our results are lower than the world average by 1.0 and 0.3 standard deviation for the $\overline{B}^0 \to D^{*+}e^-\overline{\nu}_e$ and $\overline{B}^0 \to D^{*+}\mu^-\overline{\nu}_\mu$ modes, respectively. While the uncertainties we estimate are significantly larger than those of the world average, this is the first branching-fraction measurement performed with Belle II data, and constitutes a test of the entire data production, processing, and analysis chain.

[1] B. Aubert *et al.* (*BABAR* Collaboration), Phys. Rev. **D77**, 032002 (2008), arXiv:0705.4008 [hep-ex].

[2] E. Waheed *et al.* (Belle Collaboration), Phys. Rev. **D100**, 052007 (2019), arXiv:1809.03290 [hep-ex].

[3] T. Abe *et al.* (Belle II Collaboration), (2010), arXiv:1011.0352 [physics.ins-det].

[4] E. Kou *et al.*, PTEP **2019**, 123C01 (2019).

[5] K. Akai, K. Furukawa, and H. Koiso (SuperKEKB Collaboration), Nucl. Instrum. Meth. **A907**, 188 (2018).

[6] D. J. Lange, *Proceedings, 7th International Conference on B physics at hadron machines (BEAUTY 2000): Maagan, Israel, September 13-18, 2000*, Nucl. Instrum. Meth. **A462**, 152 (2001).

[7] B. Ward, S. Jadach, and Z. Was, Nucl. Phys. B Proc. Suppl. **116**, 73 (2003), arXiv:hep-ph/0211132.

[8] T. Sjostrand, S. Mrenna, and P. Z. Skands, Comput. Phys. Commun. **178**, 852 (2008), arXiv:0710.3820 [hep-ph].

[9] G. C. Fox and S. Wolfram, Phys. Rev. Lett. **41**, 1581 (1978).

[10] M. Tanabashi *et al.* (Particle Data Group), Phys. Rev. **D98**, 030001 (2018).

[11] F. Abudinén *et al.* (Belle II Collaboration), Chin. Phys. **C41**, 021001 (2020), arXiv:1910.05365 [hep-ex].

[12] Y. S. Amhis *et al.* (HFLAV Collaboration), (2019), arXiv:1909.12524 [hep-ex].

[13] A. J. Bevan *et al.* (*BABAR* & Belle Collaborations), Eur. Phys. J. **C74**, 3026 (2014), arXiv:1406.6311 [hep-ex].

[14] J. P. Lees *et al.* (*BABAR* Collaboration), Nucl. Instrum. Meth. **A726**, 203 (2013), arXiv:1301.2703 [hep-ex].